Pre-Clinical Research Report

Journal of INTERNATIONAL MEDICAL RESEARCH

Journal of International Medical Research
48(11) 1–12

DOI: 10.1177/0300060520965809
journals.sagepub.com/home/imr
SAGE

The mechanism of curcumin post-treatment relieving lung injuries by regulating miR-21/TLR4/NF-κB signalling pathway

Hai-Bo Zou and Xiao-Feng Sun

Abstract

Objective: To investigate the mechanism by which curcumin prevents lung injury in a rat model of limb ischaemia-reperfusion injury.

Methods: Rats were randomized into four groups ($n = 20$): control group (sham group); ischaemia-reperfusion group (I/R group); curcumin group (I/R+Cur group); and inhibitor of agomir-21 group (I/R+Cur+antagomir-21 group). At 3 h after reperfusion, lung tissues were collected for histopathology and immunohistochemistry to determine the apoptosis index (AI). Lung injury score (LIS) and lung wet/dry (W/D) ratio were determined. Lung microRNA-21 (miR-21) mRNA levels were measured using reverse transcription–polymerase chain reaction. Toll-like receptor 4 (TLR4) and nuclear factor kappa-B p65 (NF-κB p65) protein levels were measured by Western blot analysis. Tumour necrosis factor (TNF)-α and interleukin (IL)-1β levels were determined by enzyme-linked immunosorbent assays.

Results: In the I/R group, the W/D, LIS, AI, miR-21 mRNA, TLR4, NF-κB p65, TNF-α and IL-1β were significantly increased and the PaO_2 was decreased compared with the sham group. Evidence of lung injury was observed in the I/R group and this was alleviated in the I/R+Cur group. An inhibitor of miR-21 (antagomir-21) reversed the protective effects of curcumin.

Conclusion: Curcumin post-treatment can alleviate the lung injuries induced by limb ischaemia-reperfusion via downregulating the levels of miR-21 mRNA.

Keywords

Curcumin post-treatment, inhibitor of agomir-21, lung, apoptosis, limb, ischaemia-reperfusion

Date received: 18 June 2020; accepted: 21 September 2020

Department of Anaesthesiology, Affiliated Central Hospital, Shenyang Medical College, Shenyang, Liaoning Province, China

Corresponding author:
Hai-Bo Zou, Department of Anaesthesiology, Affiliated Central Hospital, Shenyang Medical College, 5 Nanqixi Road, Tiexi District, Shenyang 110024, Liaoning Province, China.
Email: 30618734@qq.com

Introduction

In recent years, with the emergence and popularization of advanced surgical procedures, such as cardiopulmonary bypass, cardiopulmonary cerebral resuscitation, shock, limb replantation and organ transplantation, fresh blood reperfusion can be undertaken after tissue and organ ischaemia. However, after the ischaemia-reperfusion of tissues and organs, the injury does not stop and it may be further aggravated.[1] Organs with an abundant blood supply can even experience two phases of pathological damage. Research has shown that pulmonary injury induced by limb ischaemia-reperfusion is a complex process involving multiple signalling pathways and factors.[2,3] Previous studies have confirmed that ischaemia-reperfusion of the limbs in rats can activate the Notch2/Hes-1 signalling pathway, which ultimately leads to renal injury.[4,5] The use of curcumin post-condition can inhibit the toll-like receptor 4 (TLR4)/nuclear transcription factor κB (NF-κB) signalling pathway to reduce the lung injury induced by limbs ischaemia-reperfusion.[6] MicroRNA (miR-21) is a popular research topic in the field of cell apoptosis and it inhibits cell apoptosis.[7,8] Whether miR-21 also participates in the progress of the lung injuries remains uncertain.

The purpose of this study was to investigate the mechanism that whether curcumin post-treatment can relieve lung apoptosis induced by limb ischaemia-reperfusion via regulating miR-21 mRNA in rats.

Materials and methods

Animal model of limb ischaemia-reperfusion injury

This study was conducted in the Department of Anaesthesiology, Affiliated Central Hospital, Shenyang Medical College, Shenyang, Liaoning Province, China in accordance with the relevant animal experimental guidelines and regulations. The study received approval from the Ethics Committee of the Affiliated Central Hospital of Shenyang Medical College (no. SYXK(liao)2018-0007).

Eighty adult male Sprague–Dawley rats aged 6–8 months (China Medical University Experimental Animal Centre, Shenyang, China), weighing 250–280 g, were randomized using a random number table method to one of four groups: control group (sham group); ischaemia-reperfusion group (I/R group); curcumin group (I/R+Cur group); and inhibitor of agomir-21 (antagomir-21) group (I/R+Cur+antagomir-21 group). The rats had free access to food (LF10 rat food; Guangdong Feeding License: 2019-05073; Guangdong Medical Experimental Animal Centre, Zhanjiang, China) and water and were housed under a 12-h light/12-h dark cycle. In the sham group, the rats were only exposed to the opening surgery without the ischaemia-reperfusion process. In the I/R group, ischaemia-reperfusion was undertaken. In the I/R+Cur and I/R+Cur+antiagomir-21 groups, curcumin (dissolved in normal saline (pH: 8.0) containing 1% ethanol by mass; batch no: 86M1611V; Sigma-Aldrich, St Louis, MO, USA) was injected at a dose of 200 mg/kg via the abdominal cavity after 2 h of limb ischaemia;[9] and the other two groups received an equal volume of normal saline (pH:8.0) containing 1% ethanol by mass. In the I/R+Cur+antagomir-21 group, rats were treated with 20 μg/g antagomir-21 (Shanghai Jima Pharmaceutical Technology, Shanghai, China) administered intravenously twice a day for 3 days to ensure that they had high levels prior to the start of the experiment.

The lung injury model of limb ischaemia-reperfusion was established by clamping the bilateral femoral arteries for 2 h and then reperfusing for 3 h as described below.[10] The rats were fasted for 12 h before clamping was undertaken but were able to drink water freely. An intraperitoneal injection of 3% sodium pentobarbital 40 mg/kg was

used for anaesthesia. The right external jugular vein was catheterized to establish venous access. The skin was cut in the femoral triangle of both hind limbs and the femoral artery and vein were separated. The femoral artery was clamped near the inguinal ligament using a non-invasive micro-artery clamp, which rendered the hind limbs deficient of blood for 2 h. Then the non-invasive micro-artery clamp was loosened and the limbs reperfused for 3 h. The blood flow was monitored by an ES-1000 SPM ultrasonic blood flow meter (Hayashi Denki, Echizen, Japan). The failure to detect blood flow was regarded as the successful sign of ischaemia and the monitored blood flow was regarded as the successful criterion of reperfusion. During the experiment, 1.5 ml/kg per h normal saline (pH: 8.0) containing was infused intravenously.

Detection of PaO_2

At 3 h after reperfusion, 3 ml of carotid artery blood was collected. The arterial blood gas was immediately analysed using a Gem Premier 3000 blood gas analyser (Instrumentation Laboratory, Bedford, MA, USA) and the PaO_2 was recorded. Then the rats were sacrificed by exsanguination.

Calculation of lung wet weight/dry weight

A 1 cm^3 sample of the upper lobe tissue of the right lung was collected from each rat. The residual blood was washed out with normal saline (pH: 8.0) at 4 °C. The wet weight (W) was measured after any excess water was absorbed using filter paper. The lung sample was then dried at 80 °C for 48 h. The dry weight (D) was measured and the W/D ratio was calculated.

Immunohistochemistry

A 1 cm^3 sample of the middle lobes of the left lung of each animal was fixed in 10% neutral formalin, dehydrated in ethanol and embedded in paraffin wax. A streptavidin-biotin complex (SABC) kit (Wuhan PhD Company, Wuhan, China) and 3,3'-diaminobenzidine (DAB) immunohistochemistry was used according to the manufacturer's instructions as described below. Positive staining was identified by a brown colour in the cytoplasm. Samples of lung tissue were cut into tissue sections (4 μm). The sections were deparaffinized and rehydrated in a descending series of alcohol dilutions followed by washing twice in 10 mM phosphate-buffered saline (PBS; pH 7.3) for 5 min at room temperature. For antigen retrieval, the sections were incubated in 3% H_2O_2 in 10 mM PBS (pH 7.3) for 5–10 min at room temperature followed by three washes in distilled water. The sections were then washed in 10 mM PBS (pH 7.3) for 5 min at room temperature. Then, blocking solution containing normal serum was added by dripping onto the slide and incubated at the room temperature for 20 min. The excess blocking solution was removed. For the target protein caspase-3, primary rabbit anti-rat caspase-3 antibody (1:100 dilution; Abcam®, Cambridge, MA, USA) was added and incubated at room temperature for 1 h followed by three washes in 10 mM PBS (pH 7.3) for 2 min each. The secondary goat anti-rabbit biotinylated antibody (1:100 dilution; Abcam®, Cambridge, MA, USA) was added and incubated at 20–37 °C for 20 min followed by three washes in 10 mM PBS (pH 7.3) for 2 min each. The SABC was added for 20 min at 20–37 °C followed by four washes in 10 mM PBS (pH 7.3) for 5 min each. DAB colour development was achieved using a kit (DAB colour development kit; Shanghai Kanglang Biotechnology, Shanghai, China) according to the manufacturer's instructions followed by washing with distilled water. Haematoxylin was used as a counterstain and applied for 2 min. The sections were differentiated by hydrochloric acid and alcohol, dehydrated, sealed and examined under a light microscope (BX-41

Microscope; Olympus, Tokyo, Japan). Cells with brown staining were classified as apoptotic cells. The apoptosis index (AI) was calculated by counting 100 cells in each of five visual fields that were randomly selected from each section. The ratio of apoptotic cells in 100 cells was taken as the AI in the lung samples.

Haematoxylin and eosin straining

The lower lobes of the left lung of each animal were fixed in 10% neutral formalin, dehydrated in ethanol and embedded in paraffin wax. Tissue sections were prepared as described above and stained with haematoxylin and eosin. A lung injury score (LIS) was used to semi-quantitatively analyse the extent of lung damage, including scores for pulmonary oedema, alveolar and interstitial inflammation, alveolar and interstitial haemorrhage, atelectasis and hyaline membrane formation, using a five-point scale:[10] 0, no injury; 1, lesion range $< 25\%$; 2, $25\% <$ lesion range $\leq 50\%$; 3, $50\% <$ lesion range $\leq 75\%$; 4, lesion range $> 75\%$. For each rat, 10 high-power fields ($\times 200$ magnification) of lung tissue were randomly observed and a total LIS was the sum of the above scores.

Detection of miR-21 mRNA

A lung tissue homogenate was prepared from the lower lobes of the right lung of each animal. Total RNA was extracted from 10% lung tissue homogenate using TRIzol® reagent (Invitrogen, Carlsbad, CA, USA) according to the manufacturer's instructions. The RNA quality and quantity were assessed using a Bioanalyzer 2100 (Qcbio Science & Technologies, Shanghai, China). Reverse transcription (RT) was used to synthesize the complementary DNA for miR-21 and the internal control β-actin using gene-specific primers and an RT kit (Gene Pharma, Shanghai, China). The reverse transcription–polymerase chain reaction (RT–PCR) primer sequences were as follows (all from Gene Pharma): miR-21 mRNA (22 base pairs [bp]): upstream 5′-CGAGAACCGACCTAACG CCA-3′, downstream 5′-CAGGGTCGAG AGGCTCGCA-3′; β-actin (198 bp): upstream 5′-AACAGGAGCATACCG-3′, downstream: 5′-GACCAGGAGAGCAGC TG-3′. The PCR cycles were run on an A33982 automated thermal cycler (Thermo Fisher Scientific Company, Shanghai, China). The cycling programme for miR-21 mRNA involved preliminary denaturation at 94 °C for 2 min, followed by 35 cycles of denaturation at 95 °C for 45 s, annealing at 57 °C for 45 s, and elongation at 72 °C for 60 s, followed by a final elongation step at 75 °C for 5 min. The cycling programme for β-actin mRNA involved preliminary denaturation at 94 °C for 2 min, followed by 30 cycles of denaturation at 94 °C for 40 s, annealing at 58 °C for 45 s, and elongation at 72 °C for 60 s, followed by a final elongation step at 75 °C for 5 min. The PCR products were analysed by 2% agarose gel electrophoresis (DYY-6B Electrophoresis Meter; Beijing Liuyi Instrument Factory, Beijing, China), followed by staining with ethidium bromide and image analysis using UV light on a WP-9413 gel imager (Beijing Precision Technology Instrument Co., Ltd, Beijing, China). The relative levels of miR-21 mRNA were represented by the ratio of the grey value between the target product and β-actin using a Scion Image Analysis System version 4.0.3.2 (Apple, Beijing, China). The threshold cycle (C_T) was used to determine the relative amount of miR-21 mRNA to β-actin mRNA using the equation $2^{-\Delta CT}$ where $\Delta C_T = (C_{T\ \text{miR-21}} - C_{T\ \beta\text{-actin}})$.

Western blot analysis of TLR4 and NF-κB p65 protein

A 10% lung tissue homogenate was prepared from the middle lobes of the right lung of each animal. Total protein was

extracted (Total Protein Extraction Kit; Beijing APPLYGEN Technology, Beijing, China) from the 10% lung homogenate by centrifugation at 12000 ***g*** at 4 °C for 2 min (General Purpose Centrifuge; ThermoFisher Scientific Company) and quantified using a Pierce BCA protein assay reagent kit (Pierce Biotechnology, Rockford, IL, USA). The proteins (20 μg per lane) were separated by 10% sodium dodecyl sulphate–polyacrylamide gel electrophoresis at 100 V for 35 min. The proteins were transferred to polyvinylidene fluoride membranes (ZHUZHOU RIFENG CHEMICAL INDUSTRY, Zhuzhou, China) using electroblot apparatus at 150 V for 2 h (Nanjing Puyang Institute of Scientific Instruments, Nanjing, China). The membranes were incubated with rabbit anti-rat TLR4 or rabbit anti-rat NF-κB p65 polyclonal antibody and rabbit anti-rat β-actin polyclonal antibody (both used at a dilution 1:1000; Shanghai Enzyme Linked Biology Company, Shanghai, China) at 4 °C overnight. The membranes were washed three times for 5 min each time with Tris-buffered saline-Tween 20 (pH 7.5; Shanghai Qinxiang Technology). Alkaline phosphatase-labelled secondary antibody (dilution 1:2000; Shanghai Enzyme Linked Biology Company) was added and the membranes incubated at room temperature for 2 h. The appropriate chromogenic substrate was added and then the membranes were scanned using a Scion Image Analysis System version 4.0.3.2 (Apple) to determine the levels of TLR4 or NF-κB p65 protein. The grey value ratio of TLR4 or NF-κB p65 compared with β-actin was used to quantify the levels of TLR4 protein.

Detection of TNF-α and IL-1β protein

A 10% lung tissue homogenate was prepared by taking the upper lobes of the left lung and the levels of tumour necrosis factor (TNF)-α and interleukin (IL)-1β were determined using enzyme-linked immunosorbent assay (ELISA) kits (ThermoFisher Scientific Company). Five wells were used for each group. The TNF-α or IL-1β standard solutions and the experimental samples were added to the wells (100 μl/well) and incubated for 2 h at 37 °C. The wells were washed three times at 4 °C to wash away any unbound substances using 300 μl concentrated wash buffer from the ELISA kits (pH 7.5) (ThermoFisher Scientific Company) diluted with deionized water. A horseradish peroxidase (HRP)-linked polyclonal antibody specific for TNF-α or IL-1β was added to the wells (100 μl/well) and incubated for 1 h at room temperature. The wells were washed with wash buffer to remove unbound antibody and HRP substrate solution was added (100 μl/well) and incubated for 20 min at room temperature. Termination fluid (50 μl/well) was added, the plates gently shaken and then placed in a microplate reader (RNE-90002; Shenzhen Rongjin Technology Co., Ltd, Shenzhen, China) to measure the optical density (OD) at 450 nm. Curve Expert software (version 1.35; Beijing Science and Technology Software Co., Ltd, Beijing, China) was used to plot the standard curves and input the corresponding OD values to calculate the TNF-α and IL-1β concentrations. The minimum detectable concentrations were 0.33 mg/ml for TNF-α and 90 ng/ml for IL-1β. Intra- and interassay coefficients of variation for all ELISAs were $< 9\%$ and $< 14\%$, respectively.

Statistical analyses

All statistical analyses were performed using the SPSS® statistical package, version 13.0 (SPSS Inc., Chicago, IL, USA) for Windows®. Data that were not normally distributed are presented as the mean ± SD. One-way analysis of variance and the least significant differences *post-hoc* test was used

to compare the groups. A P-value < 0.05 was considered statistically significant.

Results

Haematoxylin and eosin staining of the lungs showed that there was hyperaemia and dilation of capillaries, thickening of alveolar septa and capillary walls, and inflammatory infiltration in the pulmonary interstitium in the I/R group compared with the sham group (Figure 1). Hyaline membrane and localized atelectasis were observed in the field of view in the I/R group. Apoptosis was observed in the I/R group. Lung injuries in the I/R+Cur group were reduced compared with the I/R group. For example, hyperaemia and oedema of the alveoli were alleviated and only a few inflammatory cells had infiltrated into the alveoli and capillaries. Lung injuries in the I/R+Cur+antagomir-21 group were aggravated compared with the I/R+Cur group. For example. the number of inflammatory cells that had infiltrated the alveoli had increased; hyperaemia and oedema were increased and hyaline membrane was observed again.

Immunohistochemistry was used to measure the levels of apoptosis in lung tissues (Figure 2). The AI increased significantly in the I/R group compared with the sham group ($P < 0.05$) (Table 1). The AI decreased significantly in the I/R+Cur group compared with the I/R group ($P < 0.05$). The AI increased significantly in the I/R+Cur+antagomir-21 compared with the I/R+Cur group ($P < 0.05$).

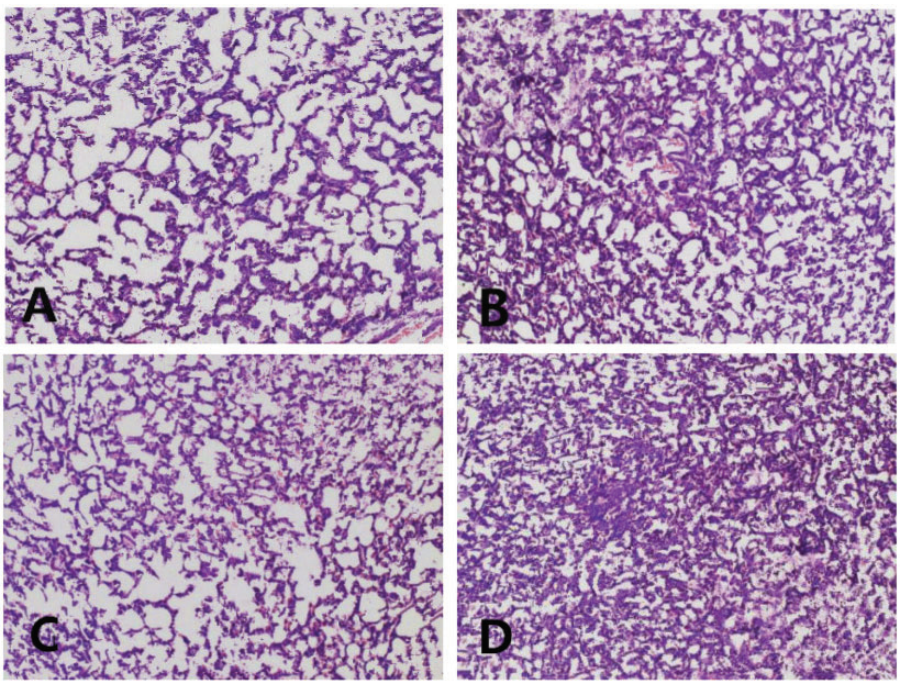

Figure 1. Representative light photomicrographs of paraffin wax-embedded sections of lung tissue showing the morphological structures in each group: (A) sham group; (B) I/R group; (C) I/R+Cur group; (D) I/R+Cur+antagomir-21 group. Sections were stained with haematoxylin and eosin. I/R, ischaemia-reperfusion; Cur, curcumin; antagomir-21, inhibitor of agomir-21. Scale bar 40 μm. The colour version of this figure is available at: http://imr.sagepub.com.

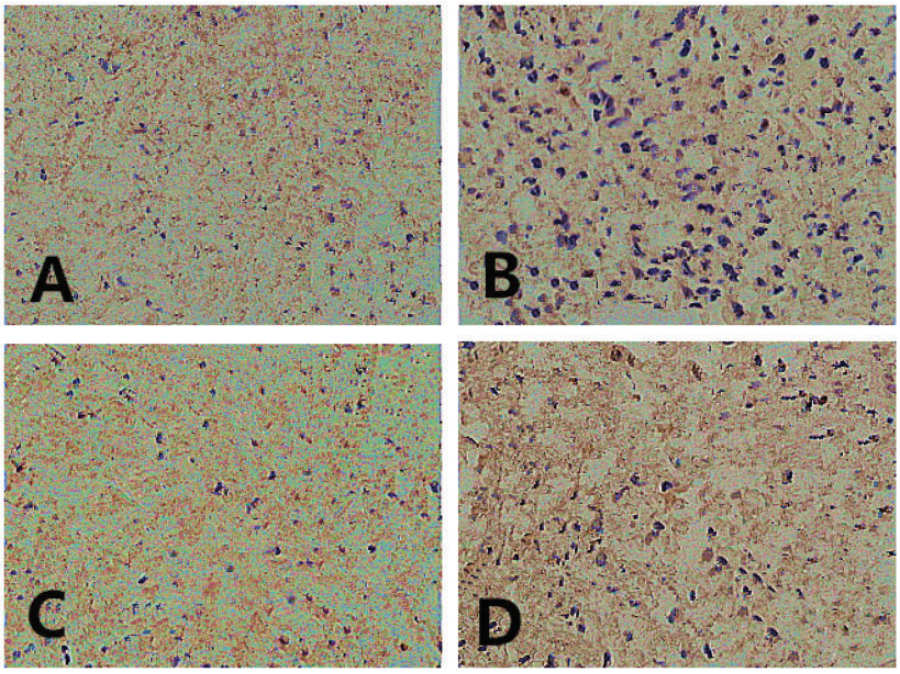

Figure 2. Representative light photomicrographs of paraffin wax-embedded sections of lung tissue showing the immunohistochemistry analysis of the levels of apoptosis in each group: (A) sham group; (B) I/R group; (C) I/R+Cur group; (D) I/R+Cur+antagomir-21 group. Sections were stained with haematoxylin and eosin. I/R, ischaemia-reperfusion; Cur, curcumin; antagomir-21, inhibitor of agomir-21. Scale bar 40 μm. The colour version of this figure is available at: http://imr.sagepub.com.

Table 1. Comparison of the measured outcomes in each group of rats.

	Measured outcomes			
Group	W/D	LIS	PaO_2, mmHg	AI, %
Sham group, $n = 20$	2.3 ± 0.2	10 ± 2	99 ± 1	33.21 ± 2.17
I/R group, $n = 20$	5.1 ± 0.3^a	21 ± 4^a	91 ± 2^a	51.03 ± 2.61^a
I/R+Cur group, $n = 20$	3.2 ± 0.2^b	13 ± 2^b	96 ± 2^b	37.71 ± 3.55^b
I/R+Cur+antagomir-21 group, $n = 20$	4.9 ± 0.3^c	19 ± 4^c	91 ± 3^c	48.03 ± 2.29^b

Data presented as mean ± SD.

$^aP < 0.05$ compared with the sham group; $^bP < 0.05$ compared with the I/R group; $^cP < 0.05$ compared with the I/R+Cur group; one-way analysis of variance and the least significant differences *post-hoc* test were used to compare the groups. W/D, wet weight/dry weight; LIS, lung injury score; PaO_2, pressure of oxygen in arterial blood; AI, apoptosis index; I/R, ischaemia-reperfusion; Cur, curcumin; antagomir-21, inhibitor of agomir-21.

The lung W/D ratio, AI and LIS significantly increased and the PaO_2 significantly decreased in the I/R group compared with sham group ($P < 0.05$ for all comparisons) (Table 1). In the I/R+Cur group, the lung W/D ratio, AI and LIS significantly decreased and the PaO_2 significantly increased compared with the I/R group

($P < 0.05$ for all comparisons). The lung W/D ratio, AI and LIS significantly increased and the PaO_2 significantly decreased in the I/R+Cur+antagomir-21 group compared with the I/R+Cur group ($P < 0.05$ for all comparisons).

The relative levels of mir-21 mRNA significantly decreased in the I/R group compared with sham group ($P < 0.05$) (Table 2 and Figure 3). The relative levels of miR-21 mRNA significantly increased in the I/R+Cur group compared with the I/R group ($P < 0.05$). The relative levels of mir-21 mRNA significantly decreased in the I/R+Cur+antagomir-21 group compared with the I/R+Cur group ($P < 0.05$).

The levels of TLR4 and NF-κB p65 proteins significantly increased in the I/R group compared with the sham group ($P < 0.05$) (Table 2 and Figure 4). The levels of TLR4 and NF-κB p65 proteins significantly decreased in I/R+Cur group compared with the I/R group ($P < 0.05$). The levels of TLR4 and NF-κB p65

Table 2. Comparison of the relative levels of microRNA-21 (miR-21) mRNA, toll-like receptor 4 (TLR4) protein and nuclear factor kappa-B p65 (NF-κB p65) protein in lung tissues in each group of rats.

Group	miR-21 mRNA	TLR4 protein	NF-κB p65 protein
Sham group, $n = 20$	2.18 ± 0.23	0.53 ± 0.02	0.31 ± 0.04
I/R group, $n = 20$	0.99 ± 0.12^a	2.78 ± 0.04^a	1.63 ± 0.03^a
I/R+Cur group, $n = 20$	2.05 ± 0.41^b	0.87 ± 0.03^b	0.45 ± 0.06^b
I/R+Cur+antagomir-21 group, $n = 20$	1.13 ± 0.27^c	2.16 ± 0.02^c	1.26 ± 0.04^c

Data presented as mean $\pm$ SD.

$^aP < 0.05$ compared with the sham group; $^bP < 0.05$ compared with the I/R group; $^cP < 0.05$ compared with the I/R+Cur group; one-way analysis of variance and the least significant differences *post-hoc* test were used to compare the groups. I/R, ischaemia-reperfusion; Cur, curcumin; antagomir-21, inhibitor of agomir-21.

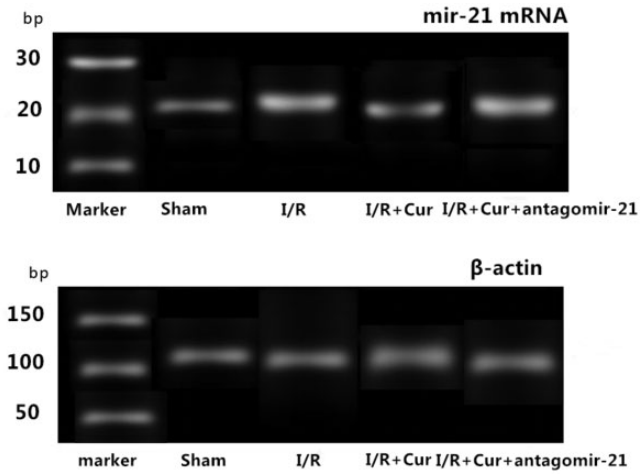

Figure 3. Representative reverse transcription–polymerase chain reaction analysis of the levels of microRNA-21 (miR-21) mRNA and the internal control gene β-actin mRNA in lung tissues in each group of rats: sham group, I/R group, I/R+Cur group and I/R+Cur+antagomir-21 group. bp, base pairs; I/R, ischaemia-reperfusion; Cur, curcumin; antagomir-21, inhibitor of agomir-21.

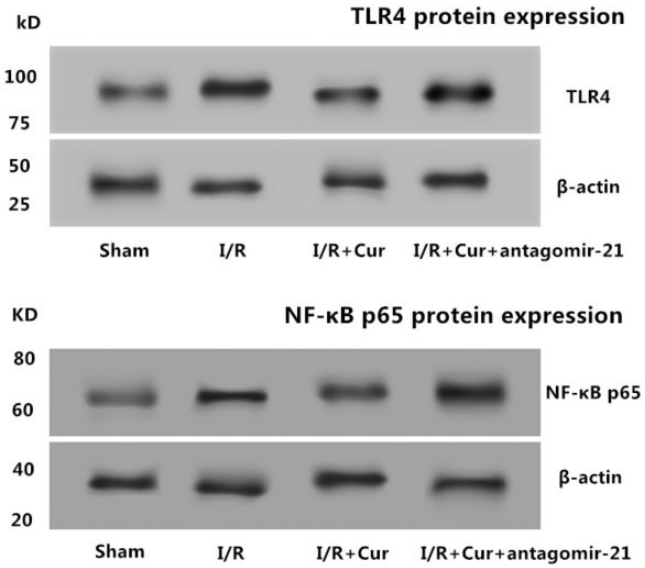

Figure 4. Representative Western blot analysis of the levels of toll-like receptor 4 (TLR4) protein and nuclear factor kappa-B p65 (NF-κB p65) protein in lung tissues in each group of rats: sham group, I/R group, I/R+Cur group and I/R+Cur+antagomir-21 group. I/R, ischaemia-reperfusion; Cur, curcumin; antagomir-21, inhibitor of agomir-21.

Table 3. Comparison of the protein levels of tumour necrosis factor-α (TNF-α) and interleukin-1β (IL-1β) in lung tissues in each group of rats.

Group	TNF-α, mg/ml	IL-1β, μg/l
Sham group, $n = 20$	1.31 ± 0.02	0.22 ± 0.04
I/R group, $n = 20$	4.29 ± 0.17^{a}	0.71 ± 0.03^{a}
I/R+Cur group, $n = 20$	1.87 ± 0.19^{b}	0.31 ± 0.05^{b}
I/R+Cur+antagomir-21 group, $n = 20$	4.03 ± 0.56^{c}	0.68 ± 0.03^{c}

Data presented as mean ± SD.
[a]$P < 0.05$ compared with the sham group; [b]$P < 0.05$ compared with the I/R group; [c]$P < 0.05$ compared with the I/R+Cur group; one-way analysis of variance and the least significant differences *post-hoc* test were used to compare the groups. I/R, ischaemia-reperfusion; Cur, curcumin; antagomir-21, inhibitor of agomir-21.

proteins significantly increased in the I/R+Cur+antagomir-21 group compared with the I/R+Cur group ($P < 0.05$).

The levels of TNF-α and IL-1β proteins significantly increased in the I/R group compared with the sham group ($P < 0.05$) (Table 3). The levels of TNF-α and IL-1β proteins significantly decreased in the I/R+Cur group compared with the I/R group ($P < 0.05$). The levels of TNF-α and IL-1β proteins significantly increased in the I/R+Cur+antagomir-21 group compared with I/R+Cur group ($P < 0.05$).

Discussion

With the development of hand and foot surgery, the patient's safety during perioperative procedures and anaesthesia has attracted considerable attention.[11] In order

to ensure a clear surgical field, it is often necessary to use a tourniquet, especially on the patient's leg during surgery. There is no doubt that the application of a tourniquet ensures a clean surgical field, but its use can lead to side-effects such as ischaemia-reperfusion injury. Moreover, this kind of injury is not only limited to the limbs, but it can also impact more distant viscera.[12] When the reperfusion phase occurs, the injurious factors that have accumulated in the affected limb will flow throughout the whole body via the blood. The blood supply to the lung is very rich and it is an essential site for gaseous exchange with the outside world. The lungs are very sensitive to noxious stimuli. A previous study showed that there were many signalling pathways participating in the progression of lung injuries induced by limb ischaemia-reperfusion.[13]

Curcumin is a chemical constituent extracted from the rhizomes of some plants of the Zingiberaceae and Araceae families.[14] Studies have shown that curcumin is the effective substance found in turmeric and it possesses various pharmacological effects, including antioxidant, antitumour and anti-inflammatory.[15–17] Among them, the anti-inflammatory and antioxidant effects of curcumin are widely recognized.[18–20]

MicroRNAs are short noncoding RNA molecules that are approximately 9–25 nucleotides long, which regulate gene transcription by binding to mRNA.[21] MiRNAs were first discovered in 1993 and since then more than 1000 miRNAs have been identified.[22] Among them, miR-21 is one of the most important because it plays an important role in tumours, cardiovascular disease, immune system diseases, the occurrence and development of epidemic diseases, endocrine diseases and nervous system diseases.[23] Research has shown that the miR-21/TLR4/NF-κB pathway takes part in myocardial apoptosis in rats with myocardial ischemia-reperfusion.[24] The current study demonstrated that the levels of miR-21 mRNA were significantly increased as a result of ischaemia-reperfusion in rats and treatment with curcumin reduced the levels of miR-21 mRNA. In addition, the concomitant administration of an inhibitor of miR-21 (antagomir-21) resulted in increased levels of miR-21 mRNA. This current study has demonstrated that curcumin post-treatment might be the up-stream initiation factor of the miR-21/TLR4/NF-κB/TNF-α and IL-1β signalling pathway, which regulate the lung cell apoptosis.

Research has shown that a large number of oxygen free radicals can activate NF-κB and the increase the release of inflammatory factors.[25] TNF-α and IL-1β are the main cytokines that initiate the inflammatory response.[26] The results of this current study showed that rats in the ischaemia-reperfusion group had evidence of inflammatory cell infiltration into their lungs and congestion/oedema of the pulmonary alveoli. The levels of TNF-α and IL-1β were significantly increased and high levels of apoptosis were seen in the rats in the ischaemia-reperfusion group. All of these results confirmed that the rat I/R model had been established successfully. Treatment with curcumin reduced the levels of lung injury, but concomitant administration of antagomir-21 resulted in increased levels of injury again. These current results strongly suggest that curcumin treatment could alleviate the lung injuries by upregulating miR-21 mRNA.

This study had several limitations. First, undertaking these preclinical experiments in rats might yield different findings compared with using human samples. As a consequence, these current findings can only serve as an indication of what might be occurring in the human situation. Secondly, the clinical application of miR-21 remains rare.

In conclusion, this current study has demonstrated that curcumin post-treatment can upregulate miR-21 mRNA levels in lung tissue and reduce the levels

of inflammatory cytokines, which alleviates the lung injury induced by limb ischaemia-reperfusion in rats.

Acknowledgements

We gratefully acknowledge the teachers of the Central Hospital Affiliated to Shenyang Medical College and the Animal Laboratory Centre of China Medical University for their strong support in this study, as well as the encouraging words given by the leaders of the hospital and the department. In addition, I would like to thank all the researchers and data collectors that participated in the actual undertaking of the study, as well as the statisticians for their help.

Declaration of conflicting interest

The authors declare that there are no conflicts of interest.

Funding

This work was supported by grants from the Research Fund for Science and Technology of ShenYang Medical College (no. 20191013), the Project Fund for Science and Technology of Liaoning Province in China (no. 20180550621), the General Projects of Liaoning Provincial Department of Education in China (no. L2015540) and the Youth Foundation Project of Shenyang Medical College (no. 20162029).

ORCID iD

Hai-Bo Zou https://orcid.org/0000-0002-8442-8113

References

1. Zou H and Sun X. Effects of cyclosporin A pre-treatment combined with etomidate post-treatment on lung injury induced by limb ischemia-reperfusion in rats. *J Int Med Res* 2020; 48. DOI: 10.1177/030006052093462.
2. Xu L, Ding L, Su Y, et al. Neuroprotective effects of curcumin against rats with focal cerebral ischemia-reperfusion injury. *Int J Mol Med* 2019; 43: 1879–1887. DOI: 10.3892/ijmm.2019.4094.
3. Xu G, Dong R, Liu J, et al. Synthesis, characterization and in vivo evaluation of honokiol bisphosphate prodrugs protects against rats brain ischemia-reperfusion injury. *Asian J Pharm Sci* 2019; 14: 640–648. DOI: 10.1016/j.ajps.2018.11.004.
4. Zou H and Sun X. Post-treatment curcumin reduced ischemia-reperfusion-induced pulmonary injury via the Notch2/Hes-1 pathway. *J Int Med Res* 2019. DOI: 10.1177/0300060519892432.
5. Du T, Zhou J, Chen WX, et al. Microvesicles derived from human umbilical cord mesenchymal stem cells ameliorate renal ischemia-reperfusion injury via delivery of miR-21. *Cell Cycle* 2020; 19: 1285–1297. DOI: 10.1080/15384101.2020.1748940.
6. Hatab HM, Abdel Hamid FF, Soliman AF, et al. A combined treatment of curcumin, piperine, and taurine alters the circulating levels of IL-10 and miR-21 in hepatocellular carcinoma patients: a pilot study. *J Gastrointest Oncol* 2019; 10: 766–776. DOI: 10.21037/jgo.2019.03.07.
7. Liu HY, Zhang YY, Zhu BL, et al. miR-21 regulates the proliferation and apoptosis of ovarian cancer cells through PTEN/PI3K/AKT. *Eur Rev Med Pharmacol Sci* 2019; 23: 4149–4155. DOI: 10.26355/eurrev_201905_17917.
8. Pan YQ, Li J, Li XW, et al. Effect of miR-21/TLR4/NF-κB pathway on myocardial apoptosis in rats with myocardial ischemia-reperfusion. *Science Eur Rev Med Pharmacol Sci* 2018; 22: 7928–7937. DOI: 10.26355/eurrev_201811_16420.
9. Sun XF and Wang J. Effects of curcumin on MMP-9/TIMP-1 balance during limb ischemia-reperfusion-induced lung injury in rats. *Chinese J Anesthesiology* 2014; 34: 474–476.
10. Wang Y, Luo J and Li SY. Nano-Curcumin Simultaneously Protects the Blood-Brain Barrier and Reduces M1 Microglial Activation During Cerebral Ischemia-Reperfusion Injury. *ACS Appl Mater Interfaces* 2019; 11: 3763–3770. DOI: 10.1021/acsami.8b20594.
11. Dutta PK. Comparison Of Epidural Dexmedetomidine And Neostigmine Used As Adjuvant To Ropivacaine In Lower

Limb Surgeries. *IOSR-JDMS* 2018; 17: 36–39.
12. Gong LR, Kan YX, Lian Y, et al. Electroacupuncture Attenuates Limb Ischemia-Reperfusion-Induced Lung Injury Via p38 Mitogen-Activated Protein Kinase-Nuclear Factor Erythroid-2-Related Factor-2/Heme Oxygenase Pathway. *J Surg Res* 2020; 246: 170–181. DOI: 10.1016/j.jss.2019.08.021.
13. Kassab AA, Aboregela AM and Shalaby AM. Edaravone attenuates lung injury in a hind limb ischemia-reperfusion rat model: A histological, immunohistochemical and biochemical study. *Ann Anat* 2020; 228:151433. DOI: 10.1016/j.aanat.2019.151433.
14. Mukherjee A, Sarkar S, Jana S, et al. Neuroprotective role of nanocapsulated curcumin against cerebral ischemia-reperfusion induced oxidative injury. *Brain Res* 2019; 1704: 164–173. DOI: 10.1016/j.brainres.2018.10.016.
15. Bavarsad K, Barreto GE, Hadjzadeh MA, et al. Protective Effects of Curcumin Against Ischemia-Reperfusion Injury in the Nervous System. *Mol Neurobiol* 2019; 56: 1391–1404. DOI: 10.1007/s12035-018-1169-7.
16. Bavarsad K, Riahi MM, Saadat S, et al. Protective effects of curcumin against ischemia-reperfusion injury in the liver. *Pharmacol Res* 2019; 141: 53–62. DOI: 10.1016/j.phrs.2018.12.014.
17. Hou Y, Wang J and Feng J. The neuroprotective effects of curcumin are associated with the regulation of the reciprocal function between autophagy and HIF-1α in cerebral ischemia-reperfusion injury. *Drug Des Devel Ther* 2019; 13: 1135–1144. DOI: 10.2147/DDDT.S194182.
18. Ni W, Yu S, Li F, et al. Renoprotective effect of curcumin labelled on Mesoscale Nanoparticles (MNPs) on Renal Ischemia-Reperfusion Injury (RIRI) via the miR-146a/nNOS/NO/cGMP/PKG signaling pathway. *Curr Pharm Biotechnol* 2019. DOI: 10.2174/1389201020666191009122035.
19. Fan Z, Yao J, Li Y, et al. Anti-inflammatory and antioxidant effects of curcumin on acute lung injury in a rodent model of intestinal ischemia reperfusion by inhibiting the pathway of NF-Kb. *Int J Clin Exp Pathol* 2015; 8: 3451–3459.
20. Hussein YA, Al-sarraf AM and Alfalluji WL. Modulation of oxidative stress, inflammatory and apoptotic response by curcumin against cerebral ischemia reperfusion injury in a mouse model. *Interdisciplinary Neurosurgery* 2020; 21: 100741.
21. Yin Z, Han Z, Hu T, et al. Neuron-derived exosomes with high miR-21-5p expression promoted polarization of M1 microglia in culture. *Brain Behav Immun* 2020; 83: 270–282. DOI: 10.1016/j.bbi.2019.11.004.
22. Li Z, Deng X, Kang Z, et al. Elevation of miR-21, through targeting MKK3, may be involved in ischemia pretreatment protection from ischemia–reperfusion induced kidney injury. *J Nephrol* 2016; 29: 27–36. DOI: 10.1007/s40620-015-0217-x.
23. Jia P, Pan T, Xu S, et al. Depletion of miR-21 in dendritic cells aggravates renal ischemia-reperfusion injury. *FASEB J* 2020. doi: 10.1096/fj.201903222RR.
24. Fang HC, Wu BQ, Hao YL, et al. KRT1 gene silencing ameliorates myocardial ischemia-reperfusion injury via the activation of the Notch signaling pathway in mouse models. *J Cell Physiol* 2019; 234: 3634–3646. DOI: 10.1002/jcp.27133.
25. Xue BB, Chen BH, Tang YN, et al. Dexmedetomidine protects against lung injury induced by limb ischemia-reperfusion via the TLR4/MyD88/NF-κB pathway. *Kaohsiung J Med Sci* 2019; 35: 672–678. DOI: 10.1002/kjm2.12115.
26. Zhang J, Tang L, Li GS, et al. The anti-inflammatory effects of curcumin on renal ischemia-reperfusion injury in rats. *Ren Fail* 2018; 40: 680–686. DOI: 10.1080/0886022X.2018.1544565.